Research Square

Preprints are preliminary reports that have not undergone peer review.
They should not be considered conclusive, used to inform clinical practice,
or referenced by the media as validated information.

Interdecadal Change in the Relationship between Summer Precipitation in Northern Southwest China and the East Asia-Pacific Teleconnection Pattern around the Early 2000s and Its Possible Causes

Jieliang Wei

3240101077@stu.cuit.edu.cn

Chengdu University of Information Technology https://orcid.org/0009-0004-9985-3763

Minggang Li

Chengdu University of Information Technology https://orcid.org/0009-0002-2015-2979

Haolin Luo

Chengdu University of Information Technology

Yong Zhao

Chengdu University of Information Technology

Pengguo Zhao

Chengdu University of Information Technology

Yang Li

Chengdu University of Information Technology

Research Article

Keywords: East Asia-Pacific Pattern, northern Southwest China, Interdecadal change, Summer precipitation

Posted Date: November 16th, 2026

DOI: https://doi.org/10.21203/rs.3.rs-11534476/v1

License: This work is licensed under a Creative Commons Attribution 4.0 International License.
Read Full License

Interdecadal Change in the Relationship between Summer Precipitation in Northern Southwest China and the East Asia-Pacific Teleconnection Pattern around the Early 2000s and Its Possible Causes

Jieliang Wei[1, 2], Minggang Li[1, 2, *], Haolin Luo[1], Yong Zhao[1, 2], Pengguo Zhao[1], Yang Li[1]

1 Climate Change and Resource Utilization in Complex Terrain Regions Key Laboratory of Sichuan Province, Chengdu Plain Urban Meteorology and Environment Observation and Research Station of Sichuan Province, Sichuan Provincial Engineering Research Center for Meteorological Disaster Prediction and Early Warning, School of Atmospheric Sciences, Chengdu University of Information Technology, Chengdu, China

2 Yunnan Key Laboratory of Meteorological Disasters and Climate Resources in the Greater Mekong Subregion, Yunnan University, Kunming, China

*Submitted to **Climate Dynamics***

Oct-2026

Corresponding to Minggang Li(limg@cuit.edu.cn); Yong Zhao (zhaoy608@cuit.edu.cn)

Abstract:

Recent studies have documented a diminished effect of the East Asia-Pacific (EAP) pattern on summer rainfall in eastern China since the early 2000s. This research extends this understanding to Southwest China, a less-studied region. The interdecadal weakening of the relationship between summer precipitation in northern Southwest China (NSWSP) and the EAP pattern is primarily due to the eastward shift of EAP-related anomalous circulation, driven by changes in diabatic heating anomalies from the Indochina Peninsula to the Central Pacific. In addition, circulation anomalies around the South China Sea bridge this NSWSP-EAP linkage. From 1970 to 2002, the tropical diabatic heating anomaly that excites the EAP pattern was stronger and located farther west, favoring intensification and westward expansion of EAP-related anomalous circulation. In particular, the EAP-driven anomalous anticyclone at lower latitudes extended beyond the South China Sea, favoring a westward-extended western Pacific subtropical high (WPSH) that transports moisture from the South China Sea and the western Pacific to northern Southwest China and induces low-level convergence there. In contrast, the heating anomaly shifted farther east during 2004–2023, producing a weaker, more eastward-located anticyclone at lower latitudes that exerted less influence on the WPSH and on the circulation over the South China Sea, thereby weakening the connection between the EAP pattern and both the NSWSP and the WPSH. Our results improve understanding of the mechanism and climate impacts of the interdecadal change in the EAP pattern and provide new insights into the enhanced interannual variability of the NSWSP since the early 2000s.

Keywords: East Asia-Pacific Pattern; northern Southwest China; Interdecadal change; Summer precipitation

1. Introduction

Northern Southwest China lies within the upper Yangtze River Basin. Its western area borders the Tibetan Plateau and has higher elevations, while its eastern part has lower-lying terrain and forms the Sichuan Basin, one of China's four largest basins (see Fig. 1a). The region has complex terrain and lies at the intersection of the East Asian summer monsoon, the South Asian summer monsoon, and the Tibetan Plateau monsoon (Yuan et al. 2018; Zhang 2020; Zhang et al. 2025), resulting in pronounced summer rainfall variability and susceptibility to disasters such as droughts, floods,

landslides, and mudslides (Xie et al. 2022; Wang et al. 2023). In recent decades, Southwest China has experienced overall warming and drying, marked by declining annual precipitation and more frequent droughts and heatwaves (Ma et al. 2013; Dong et al. 2025; Wang et al. 2025). However, extreme precipitation events and their share of annual rainfall have increased (Xiao et al. 2018; Zheng et al. 2022), leading to more frequent floods and, together with the drying trend, more frequent droughts (Bi et al. 2023; Li et al. 2026). This climate background also fosters various compound extreme events, including rapid transitions between drought and flood (Yu et al. 2023; Qiu et al. 2024; Su et al. 2024; Wu et al. 2026), all of which threaten residents' safety and property and underscore the importance of improving climate forecasting capabilities.

Because Southwest China is located in a region influenced by three monsoon systems, sea surface temperature anomalies (SSTAs) in the major oceans can affect its summer rainfall by altering monsoon-related moisture transport (Zhang et al. 2017; Sun et al. 2024) or by modifying monsoon components such as the South Asian High (SAH, Liu et al. 2013; Luo and Yang 2024), the western Pacific subtropical high (WPSH, Yan and Wang 2019), and the East Asian Jet Stream (EAJ, Wang and Zuo 2016). For example, Zhang et al. (2017) noted that water vapor fueling summer rainfall in Southwest China mainly originates from the west and east, driven by the South Asian and East Asian summer monsoons, respectively. Moreover, SST-induced convective anomalies over the tropical western Pacific can excite Rossby wave responses and trigger teleconnection patterns that propagate towards East Asia, thereby establishing a dynamical link between ocean variability and Asian summer monsoon rainfall anomalies (Yang et al. 2022; Noh et al. 2023; Li et al. 2024). For instance, Sun et al. (2024) found that the late-summer Indo-Pacific SST gradient can trigger westward-propagating Rossby waves, creating an anticyclonic shear zone over the western subtropical Pacific and increasing rainfall in Southwest China. Furthermore, Yang et al. (2022) noted that the East Asia-Pacific teleconnection can influence summer rainfall variability over Southwest China by modulating the WPSH and water vapor transport.

The East Asia-Pacific teleconnection pattern (EAP, Huang and Li 1987), also known as the Pacific-Japan pattern (PJ, Nitta 1987), is characterized by a Rossby wave train triggered by anomalous convective activity around the Philippines. It propagates meridionally towards the Sea of Okhotsk and plays a key role in regulating

the East Asian summer monsoon (Huang and Sun 1992; Ding and Chan 2005; Kosaka and Nakamura 2006, 2010). The positive phase of the EAP wave train typically comprises an anomalous anticyclonic circulation over the subtropical Northwest Pacific, an anomalous cyclonic circulation from the Yangtze-Huai River valley to Japan, and an anomalous anticyclonic circulation over the Okhotsk Sea (Huang 2004; Kosaka and Nakamura 2010; Wu et al. 2013; Xie et al. 2016). These features are associated with variations in the intensity and position of the WPSH and EAJ (Ding and Chan 2005; Fujinami and Yasunari 2009; Wang et al. 2018; Hu et al. 2024; Liu et al. 2024; Wang and Xu 2024). Consequently, the EAP pattern strongly influences summer rainfall over East Asia, notably during the Meiyu/Baiu/Changma periods (Li et al. 2016; Shang et al. 2020; Yu et al. 2026; Sun et al. 2026). SSTAs in tropical oceans can influence the pattern's variability (Huang and Li 1988; Qu and Huang 2012; Lin et al. 2021; Yang et al. 2025). In particular, the capacitor effect (Xie et al. 2009) describes the connection between winter warming in the eastern tropical Pacific (EP El Niño), spring and summer warming in the tropical Indian Ocean (Indian Ocean basin mode, IOBM), and the formation of an anomalous anticyclonic circulation over the subtropical Northwest Pacific. This anomalous anticyclone links Indo-Pacific SSTAs with the EAP pattern via interactions with convective activity around the Philippines (Wang et al. 2000; Yang et al. 2007; Wu et al. 2010; Xie et al. 2016; Huangfu et al. 2018; Kosaka et al. 2021; Song et al. 2025).

The capacitor effect involves a complex chain of interactions, where even minor changes in one link can cause significant shifts in the EAP pattern (Sun et al. 2014; Kubota et al. 2016; Tao et al. 2017). Recent studies have documented an interdecadal change in the EAP pattern around the early 2000s, offering insights into the underlying mechanisms. For example, Xu et al. (2019) observed a notable eastward shift and weakening of the EAP's barotropic structure in the extratropics since the late 1990s, attributing this to a change in the excitation location of the EAP wave train. Li and Lu (2020) suggested that background SST changes since the early 2000s have weakened the meridional connection between the western North Pacific and East Asia. One proposed mechanism is that during the decaying phase of the central Pacific El Niño, cooling in the tropical Pacific without significant warming in the tropical Indian Ocean during boreal summer offsets the southward shift of the EAJ driven by tropical western North Pacific convection, thereby disrupting the tropical-subtropical seesaw pattern. Lu et al. (2022) proposed that a weakened EAP pattern since the mid-2000s,

driven by notable changes in sea surface temperature differences between the tropical eastern-central Pacific and the western Pacific, explained the decline in the relationship between summer precipitation variability over South China and the EAP pattern. Sun et al. (2024) found that the strong correlation between IOBM and the EAP pattern disappeared after 2006 because PJ-C (the Northeast Asian anomalous cyclone of the PJ pattern) and IOBM decoupled, likely due to a shift in oceanic forcing from the IOBM to SSTAs in the central/eastern Pacific. Huang et al. (2025) reported that the main driver of marine heatwaves in the East Sea/Japan shifted from the EAP pattern to the Eurasian teleconnection around 2001, possibly related to increased impacts of North Atlantic SSTAs. These studies improve our understanding of the mechanisms driving the interdecadal change in the EAP pattern around the early 2000s.

Although the mechanism underlying this interdecadal shift in the EAP pattern remains uncertain, the EAP pattern's diminished influence on the summer climate of eastern China and Japan is well documented (Xu et al. 2019; Li and Lu 2020; Huang et al. 2025). In contrast, the interannual relationship between the EAP pattern and summer rainfall in Southwest China, as well as the effects of long-term changes in the EAP pattern on summer rainfall there, remain underexplored. Therefore, this study aims to address two main questions: 1) how the EAP pattern affects summer rainfall over northern Southwest China, and 2) why the notable connection between the EAP pattern and summer rainfall over northern Southwest China (NSWSP) has diminished over the past two decades. These results will improve our understanding of the mechanisms driving EAP variation and provide new insights into recent climate variability in Southwest China. The rest of this paper is organized as follows: Section 2 details the data sources and methods; Section 3 presents our key findings, including two subsections: 3.1 shows statistical evidence of the interdecadal change in the NSWSP-EAP relationship; 3.2 explores possible physical mechanisms behind this change. Section 4 compares the results with the existing literature. Finally, Section 5 concludes the study.

2. Data and Methods

2.1 Data

This study covers the period 1970–2023. The data sources are listed below:

(1) CHM_PRE V2 monthly precipitation grid data for mainland China at a horizontal resolution of 0.1° × 0.1°. This newly developed high-resolution gridded

dataset is based on more than 3,400 observation gauges in mainland China and incorporates 11 precipitation-related variables (Hu et al. 2025). We compared it with CN05.1 grid data (Wu and Gao 2013), and the results show limited bias in both the spatial (Fig. 1b) and temporal (Fig. 1c) dimensions across northern Southwest China.

(2) ERA5 monthly mean reanalysis data with a horizontal resolution of 0.25° × 0.25° from the European Center for Medium-Range Weather Forecasts (Hersbach et al. 2020).

(3) Outgoing longwave radiation (OLR) data (Liebmann and Smith 1996) with a horizontal resolution of 2.5° × 2.5°, provided by the National Oceanic and Atmospheric Administration (NOAA).

(4) Sea surface temperature (SST) data with a horizontal resolution of 1.0° × 1.0° from the UK Met Office Hadley Center (Rayner et al. 2003).

The climatology in this study is the 1970–2023 summer mean, with summer defined as June-July-August. In Figs. 3–6 and 8–9, the linear trend was removed from both the indices and the atmospheric fields before regressions were computed for each sub-period.

2.2 Climate indices

The indices for Eastern Pacific El Niño (EP El Niño) and Central Pacific El Niño (CP El Niño) were computed from SSTAs in the Niño 3 and Niño 4 regions, respectively, obtained from the NOAA Climate Prediction Center (CPC). The EAP teleconnection pattern index was calculated from ERA5 reanalysis data, following Xie et al. (2016). It is defined as the leading EOF mode of the 850-hPa zonal wind (scaled by the Coriolis parameter) over the Northwest Pacific.

We also used three indices to characterize variations in the western Pacific subtropical high (WPSH) and its relationship to the NSWSP and EAP pattern (Table 1): the area index, intensity index, and western ridge point index. These indices are based on the 500 hPa geopotential height field and are issued by the National Climate Center of the China Meteorological Administration. Specifically, the area index is the number of grid points with heights of at least 5880 gpm within 10°N–60°N, 110°E–180°; the intensity index is the sum of grid points with heights above 5870 gpm over the same region; and the western ridge point index is the longitude of the westernmost 5880 gpm contour within 10°N–60°N, 90°E–180°.

2.3 Numerical experiment

To verify the atmospheric response to tropical diabatic heating anomalies across

two epochs, we use the linear baroclinic model (LBM) developed by Watanabe and Kimoto (2000), which performs well in simulating the East Asian summer monsoon and climate (Tao et al. 2016; Lin and Bueh 2021). By linearizing the primitive equations about a designated background state, the LBM excludes nonlinear dynamics, such as convective feedbacks. This simplified setup isolates the direct atmospheric dynamical adjustment driven by a prescribed diabatic heating source, providing a reliable tool for evaluating circulation shifts triggered by anomalous latent heating. Here, the LBM is run with a T42 horizontal truncation and 20 unevenly spaced vertical σ levels. We integrate the model for 30 days and compute the average over the final 10 days for diagnostic evaluation.

In this study, two sets of experiments (comprising four individual runs, named R_1A, R_1B, R_2A, and R_2B) were conducted. In the first set, the spatial scope of the input fields (110°E–160°E, 10°N–20°N) was consistent across the two trials. Specifically, R_1A employed the EAP-related three-dimensional heating anomaly from epoch 1, whereas R_1B utilized the field from epoch 2. Given the significant discrepancy in heating-anomaly intensity over regions west of the Philippines between these two epochs (see the more detailed discussion in Section 3.2.2), the first set of experiments was primarily designed to examine how variations in heating intensity affect the EAP pattern. For the second set, R_2A applied the epoch-1 heating anomaly over a region mainly west of the Philippines (110°E–140°E, 10°N–20°N), and R_2B applied the epoch-2 heating anomaly over a region mainly east of the Philippines (130°E–160°E, 10°N–20°N). This group of experiments was designed primarily to examine how variations in heating location affect the EAP pattern, since the two input fields differ little in intensity.

3. Results

3.1 Statistical evidence for the interdecadal change in the NSWSP-EAP relationship

Previous studies have noted the influence of the EAP pattern on the summer climate of Southwest China (Xu et al. 2021; Yang et al. 2022). For example, Li et al. (2025) reported a significant interannual connection between the EAP pattern and summer extreme wet spells over the West Sichuan Plateau (the western part of northern Southwest China) and a weaker connection over the Sichuan Basin (the eastern part of northern Southwest China), indicating that the EAP pattern can affect summer precipitation across northern Southwest China. We calculated the correlation

between the EAP index and summer precipitation across Southwest China from 1970 to 2023. The results (not shown) indicate a significant positive correlation across most of northern Southwest China, suggesting that the EAP pattern can influence summer precipitation over much of the region.

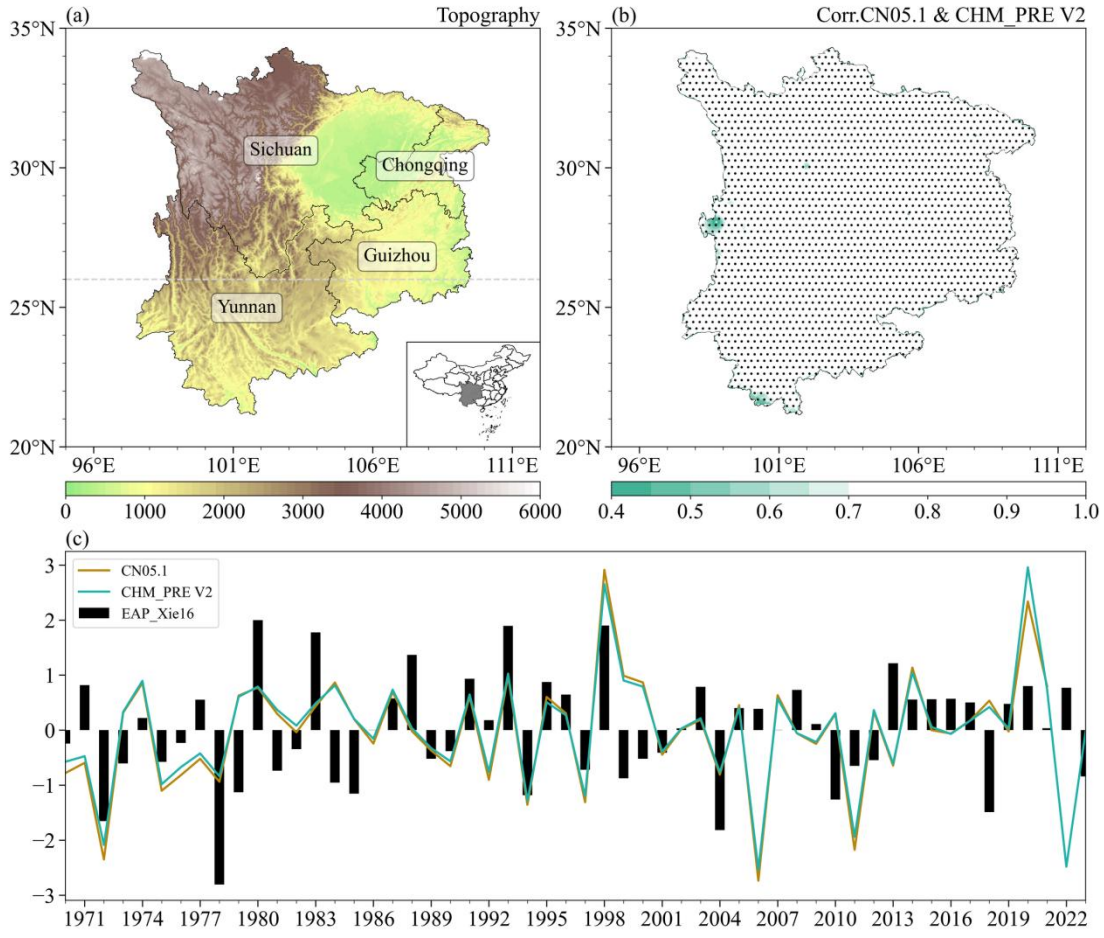


Fig. 1 (a) Geographic location and topography (shading) of Southwest China. (b) Correlation coefficients between the CHM_PRE V2 and CN05.1 datasets for total summer precipitation at each grid point across Southwest China from 1970 to 2022, with dotted regions indicating statistical significance at the 95% confidence level. (c) Standardized anomalies of the EAP index (bars) and the regional mean total summer precipitation (lines) over northern Southwest China from 1970 to 2023.

However, on interdecadal timescales, the relationship between two climate factors often changes (Liu et al. 2022; Wang et al. 2023; Zhi et al. 2025). As shown in Fig. 1c, synchrony between NSWSP and the EAP index has markedly declined since the early 2000s. A sliding correlation analysis (Fig. 2a) and a Fisher r-to-z transformation confirm this change. The strong positive correlation between NSWSP and the EAP pattern disappeared around 2002/2003 (Fig. 2a). By splitting the study period into two

epochs, 1970–2002 (epoch 1) and 2004–2023 (epoch 2), the r-to-z test indicates that the change in the NSWSP-EAP correlation is significant at the 90% confidence level ($Z = 1.825$, $p = 0.068$). In addition, this interdecadal shift is a regional phenomenon in northern Southwest China. During epoch 1, the EAP pattern was significantly associated with summer rainfall over most of northern Southwest China (Fig. 2b), whereas this significant positive link narrowed to a small area in northwestern Yunnan Province during epoch 2 (Fig. 2c).

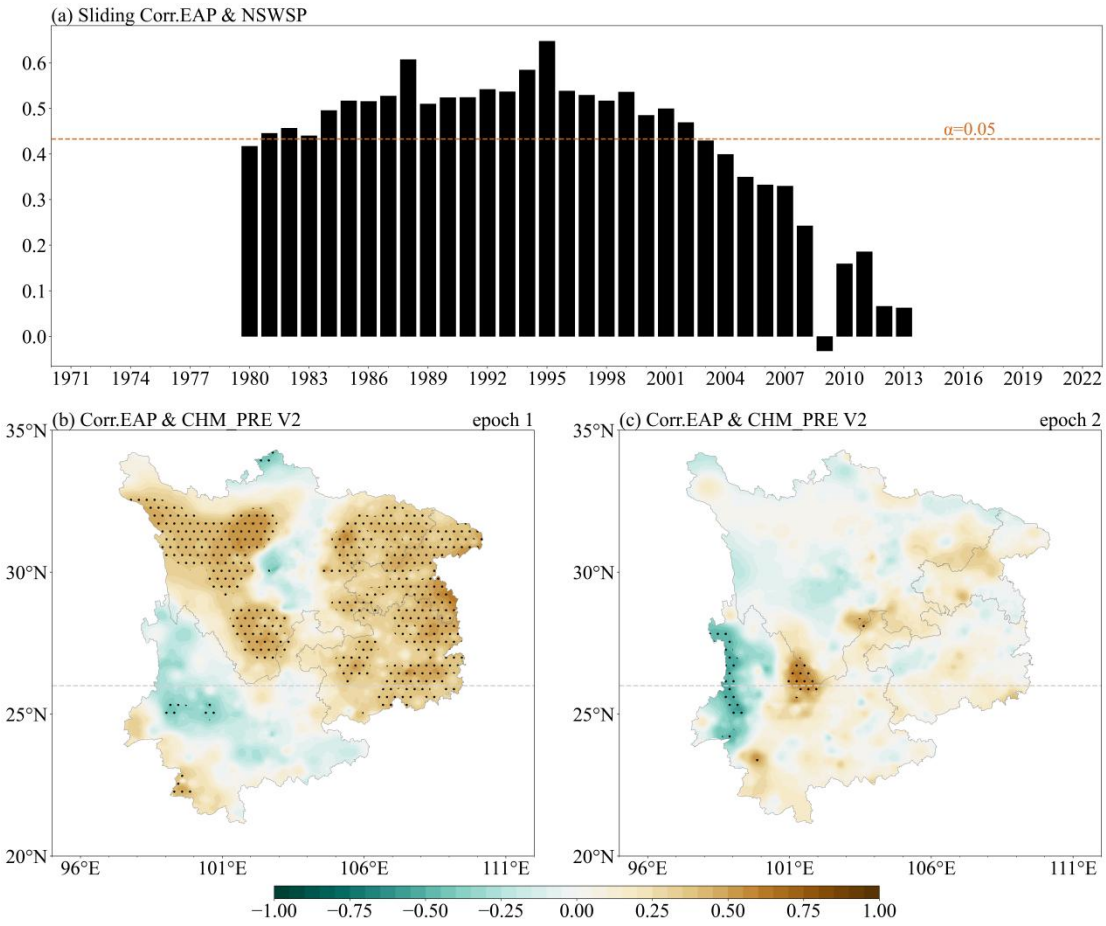


Fig. 2 (a) Sliding correlation coefficients between the EAP index and the regional mean total summer precipitation over northern Southwest China, computed with a 21-year window from 1970 to 2023. Correlation coefficients between the EAP index and CHM_PRE V2 total summer precipitation across Southwest China during (b) epoch 1 and (c) epoch 2, with dotted regions indicating statistical significance at the 95% confidence level.

The reduced influence of the EAP pattern may have contributed to greater interannual variation in NSWSP. The interannual variability of the NSWSP changed markedly between the two epochs, while the total amount remained relatively stable throughout the study period (Fig. 1c). The standard deviation of the regional average

NSWSP increased from 50.4 mm in epoch 1 to 70.6 mm in epoch 2, a statistically significant difference at the 90% confidence level (F-test). In contrast, the standard deviation of the EAP index decreased from 1.09 to 0.84 between the epochs, which is also statistically significant.

3.2 Possible causes for the interdecadal change in the NSWSP-EAP relationship

3.2.1 Changes in the circulation background associated with NSWSP interannual variability

The analysis above shows that the interdecadal change in the NSWSP-EAP relationship is robust and statistically significant. To investigate potential causes, we first examined changes in the large-scale circulation associated with NSWSP interannual variation. Significant differences between the two periods are apparent over the region extending from the Maritime Continent northward to the Sea of Okhotsk, along which the EAP pattern typically propagates (Fig. 3). During epoch 1, the EAP pattern was evident in the regression of horizontal winds and vorticity onto standardized NSWSP in the lower (700 hPa; Fig. 3a) and middle troposphere (500 hPa; not shown). These include significant anomalous anticyclonic circulation (negative vorticity anomalies) over regions from the Indochina Peninsula to the northwest Pacific, significant anomalous cyclonic circulation (positive vorticity anomalies) over regions from North China to the Japan Sea, and significant anomalous anticyclonic circulation (negative vorticity anomalies) across most of the Russian Far East. The first two anomalous circulation systems can induce anomalous convergence across most of the Yangtze River basin in the middle and lower troposphere, thereby explaining the significant NSWSP-EAP correlations during this period (e.g., Fig. 2b). By contrast, during epoch 2, the regression map shows no significant signs of the EAP pattern in the lower (Fig. 3b) and middle troposphere. Instead, anomalous westerly winds on the southern side of the Tibetan Plateau transport anomalous water vapor from the northern Indian Ocean to Southwest China, thereby enhancing summer precipitation there. In the upper troposphere (200 hPa; Fig. 3c-d), anomalous anticyclonic circulation over the region from the northern Indian Peninsula to South China and the accompanying anomalous divergence belt along 30°N are evident in both epochs, favoring convective activity over the northern part of Southwest China, even though both the anomalous anticyclone and the divergence belt are comparatively weaker during epoch 2.

Consistent with the weakening of the anomalous anticyclonic circulation over the

South China Sea (Figs. 3a-b), anomalous descent in this region also decreased from epoch 1 to epoch 2 (not shown). This weakened link between NSWSP and the anomalous anticyclone over the South China Sea reduced the transport of anomalous water vapor from the Northwest Pacific and the South China Sea into northern Southwest China. Consequently, the water vapor convergence belt along 30°N weakened substantially during epoch 2 (Figs. 3e-f).

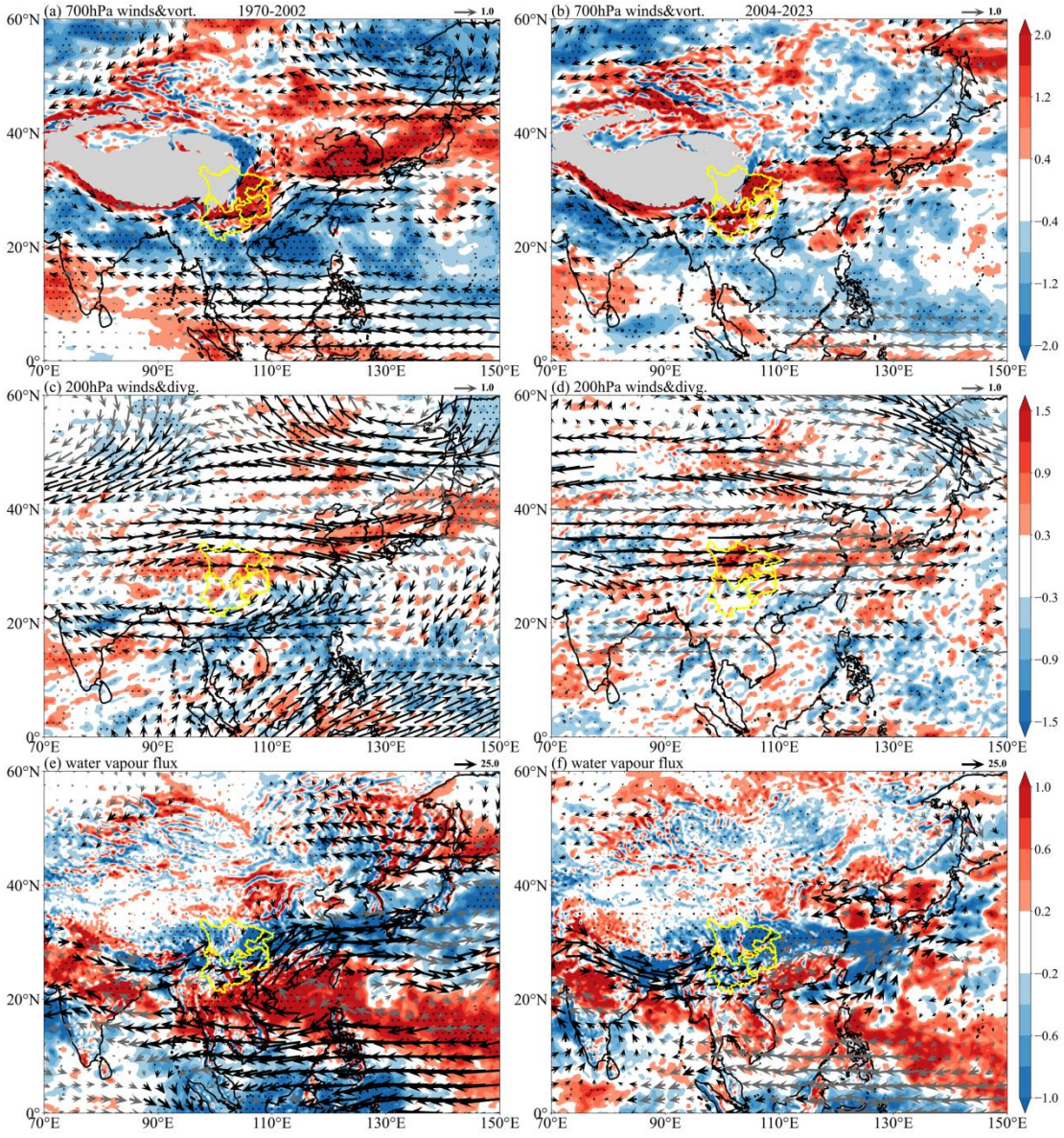


Fig. 3 Regression of horizontal winds (vectors; m s^{-1}) and vorticity (shades; 10^{-6} s^{-1}) at 700 hPa onto standardized summer precipitation over northern Southwest China during (a) epoch 1 and (b) epoch 2. (c) and (d) are as in (a) and (b), respectively, but for horizontal winds (vectors; m s^{-1}) and their divergence (shades; 10^{-6} s^{-1}) at 200 hPa. Regression of vertically integrated (from the surface to 300 hPa) water vapor fluxes (vectors; kg m^{-1} s-1) and their divergence (shades; 10^{-5} kg m^{-2} s^{-1}) onto standardized summer precipitation over northern Southwest China during (e) epoch 1 and (f) epoch 2. Dark arrows and shaded dots denote statistical significance at the 90% confidence

level for the t-test.

Variations in atmospheric heating, indicated by OLR and diabatic heating (Q1; Yanai et al. 1973), can explain the main shifts in the associated anomalous circulation pattern observed between epochs 1 and 2. First, both the regressed OLR (Figs. 4a-b) and Q1 (Figs. 4c-d) show significant signals over the region from the Indochina Peninsula to the Philippines only in epoch 1. The positive OLR anomaly and negative Q1 anomaly indicate suppressed convection, supporting the development and persistence of the anomalous anticyclonic circulation over the South China Sea during epoch 1. Second, from epoch 1 to 2, the negative Q1 anomaly over the ocean east of the Philippines weakens markedly (Figs. 4c-d), whereas the positive Q1 anomaly from North China to Japan shifts to negative anomalies, with reduced consistency. These changes hinder the formation of the anomalous anticyclonic circulation at lower latitudes and of the anomalous cyclonic circulation at middle latitudes, respectively, explaining the disappearance of the EAP signal and the weakening of the anomalous convergence along 30°N in epoch 2.

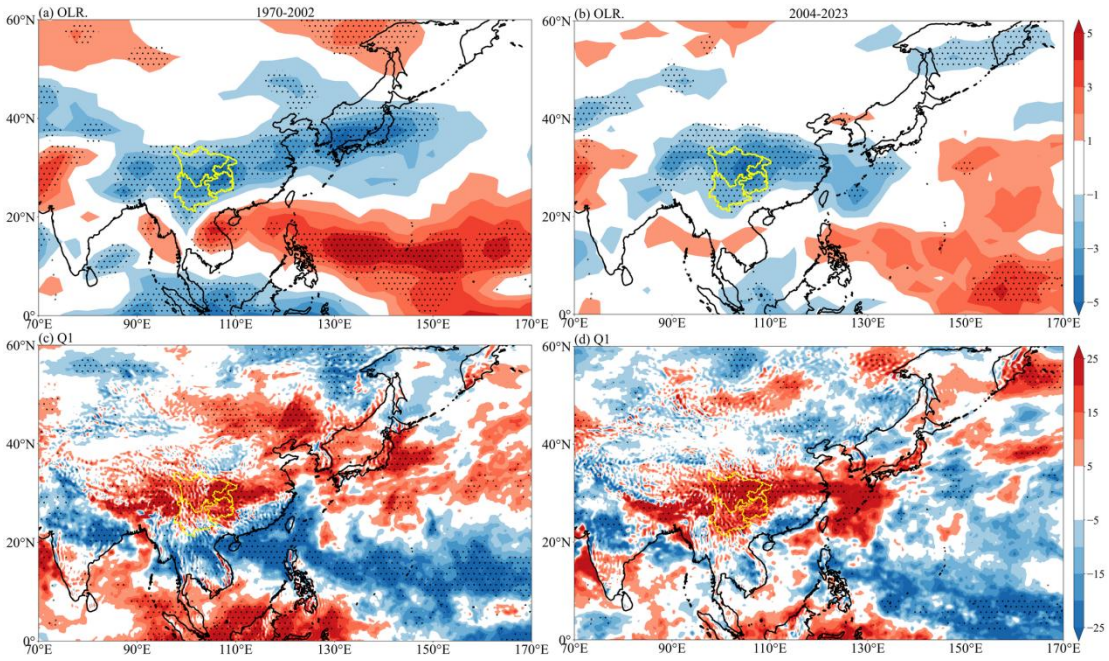


Fig. 4 Regression of outgoing longwave radiation (W m^{-2}) onto standardized summer precipitation over northern Southwest China during (a) epoch 1 and (b) epoch 2. (c) and (d) are as in (a) and (b), respectively, but for vertically integrated diabatic heating (from the surface to 100 hPa, W m^{-2}). Shaded areas with dots indicate statistical significance at the 90% confidence level for the t-test.

The South China Sea region exhibited the most pronounced thermal and dynamic

changes between the two periods, making it a useful diagnostic of the EAP pattern's influence on NSWSP. During epoch 1, strong diabatic heating anomalies near the Philippines supported EAP wave-train excitation and favored WPSH enhancement and westward extension, thereby inducing the anomalous circulations observed over the South China Sea (e.g., Figs. 3–4). By contrast, during epoch 2, diabatic heating anomalies near the Philippines were markedly weaker, suppressing EAP excitation and the intensification and expansion of the WPSH. As a result, anomalous descent and the low-level anticyclone over regions from the Indochina Peninsula to the Philippines were weak and insignificant.

3.2.2 Interdecadal change in the EAP pattern and its possible causes

To identify possible causes of the weakened NSWSP-EAP relationship, we further examined changes in EAP-related anomalous circulation and diabatic heating between epochs 1 and 2. Figs. 5a-b show the regression of horizontal winds and vorticity onto the standardized EAP index for the two epochs. The EAP-associated anomalous circulation changed significantly from epoch 1 to epoch 2, with reduced intensity of the three anomalous centers and a contraction of the area they influenced, consistent with Xu et al. (2019). During epoch 1 (Fig. 5a), EAP-related anomalous anticyclonic circulation influenced regions from the Indochina Peninsula to the Northwest Pacific, while anomalous cyclonic circulation affected regions from North China to Japan. During epoch 2 (Fig. 5b), EAP-induced anomalous vorticity weakened significantly over regions from the Indochina Peninsula to the South China Sea, North China, and the Russian Far East. Consequently, the western edges of the two anomalous circulation systems over the middle to lower latitudes retreated eastward, reducing direct control over Southwest China, and anomalous moisture transport along the western edge of the WPSH was less likely to reach and converge over northern Southwest China. As shown in the regressed anomalous vertical circulation averaged from 110°E to 140°E (Figs. 5c-d), anomalous descent at 20°N is evident in both epochs, whereas significant anomalous ascent at 30°N occurs only in epoch 1. Over lower latitudes, as depicted by the regressed anomalous vertical circulation averaged from 10°N to 25°N (not shown), the significant anomalous descent from the Indochina Peninsula to the South China Sea diminished from epoch 1 to epoch 2. The zonal and meridional mean vertical circulations also indicate a significant weakening of the two EAP-related anomalous systems in the mid-to-low latitudes. In summary, the two anomalous circulation systems associated with the EAP pattern over the lower

and middle latitudes were more intense and extended farther westward, and northern Southwest China was directly influenced by anomalous low-level convergence induced by these two systems during epoch 1. As these two anomalous systems moved away from northern Southwest China during epoch 2, the linkage between NSWSP and the EAP teleconnection pattern weakened significantly.

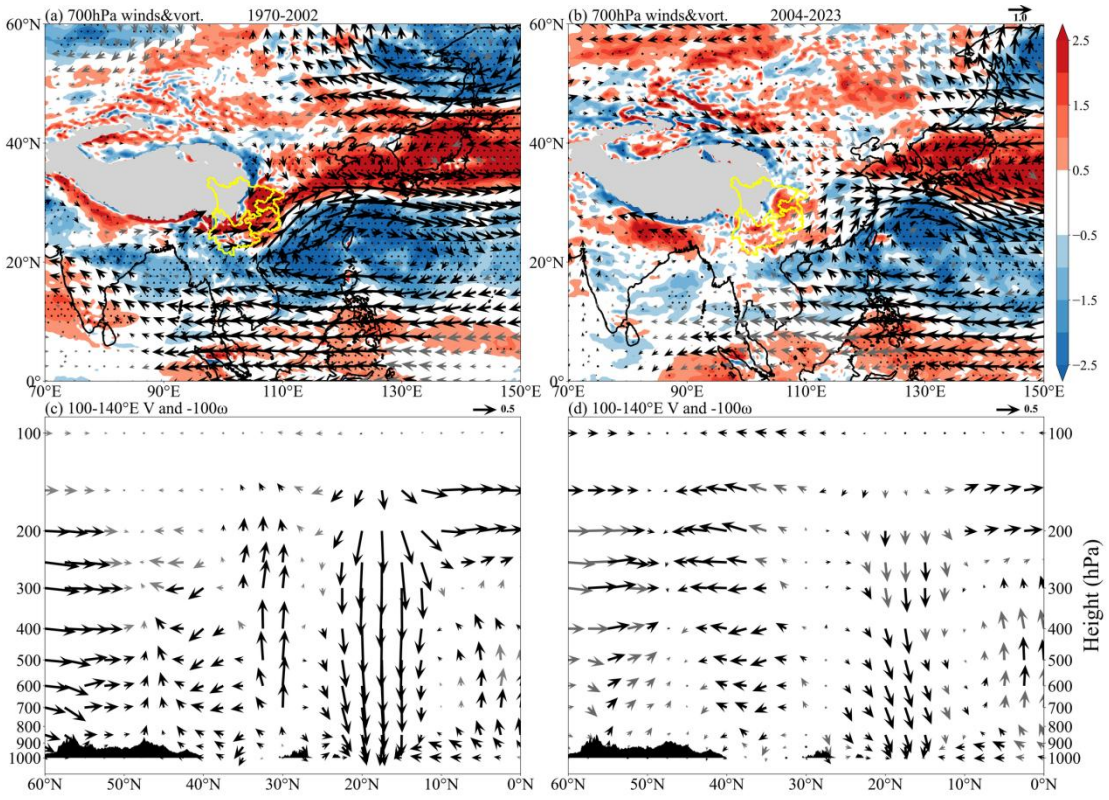


Fig. 5 Regression of horizontal winds (vectors; m s^{-1}) and vorticity (shading; 10^{-6} s^{-1}) at 700 hPa onto the standardized EAP index during (a) epoch 1 and (b) epoch 2. (c) and (d) are as in (a) and (b), respectively, but for vertical circulation, expressed as V and -100ω, averaged between 100°E and 140°E. Dark arrows and shaded dots indicate statistical significance at the 90% confidence level for the t-test.

The regressed atmospheric heating fields provide clues about the interdecadal change in the EAP pattern and the weakening of its influence on NSWSP since the early 2000s. Consistent with the eastward contraction of EAP-related anomalous circulation from epoch 1 to epoch 2, significant positive OLR anomalies over the South China Sea and significant negative OLR anomalies from northern Southwest China to the Japan Sea weakened markedly (Figs. 6a-b). These OLR anomalies corresponded to anomalous low-level anticyclonic circulation around the South China Sea and anomalous ascent across the Yangtze River valley, respectively, both of which benefited summer precipitation over northern Southwest China. Changes in the

regressed Q1 between the two epochs (Figs. 6c-d) explain the weakening and eastward shift of the three anomalous centers of the EAP pattern well. During epoch 1, notable negative Q1 anomalies appeared from the Indochina Peninsula eastward to the Central Pacific and from the Russian Far East to the Sea of Okhotsk, while significant positive Q1 anomalies appeared from North China to the oceans east of Japan. These heating anomalies support the formation and maintenance of the three EAP centers, leading to a strong EAP signal. In epoch 2, the magnitude of negative Q1 anomalies from the Indochina Peninsula to the Philippines and of positive anomalies from North China to the Japan Sea decreased markedly. The negative anomalies from the Russian Far East to the Sea of Okhotsk also weakened significantly and became regionally inconsistent. These changes limited the westward extension of the three anomalous circulation centers associated with the EAP pattern. Consequently, the EAP signal weakened significantly across East Asia.

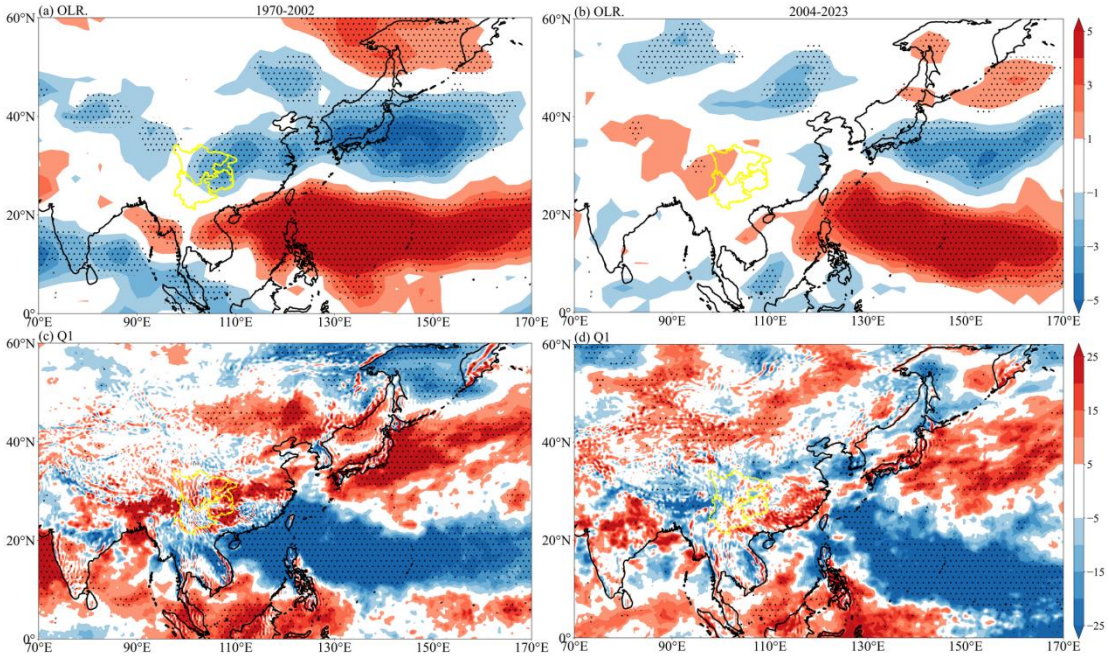


Fig. 6 Same as Fig. 4, but for regression onto the EAP index.

In contrast, the interdecadal change in the NSWSP-related circulation background (Figs. 3–4) from epoch 1 to 2 shows a vanishing EAP signal, whereas the EAP-linked change (Figs. 5–6) involves an eastward contraction of the EAP wave train. Both are associated with changes in diabatic heating anomalies across regions from the Indochina Peninsula eastward to the Central Pacific. These changes in anomalous diabatic heating have two components: a robust decrease west of the Philippines and a weak increase east of the Philippines. Therefore, we conducted two groups of

numerical experiments to assess how changes in the intensity (Figs. 7a-b) and location (Figs. 7c-d) of the tropical diabatic heating anomaly affect the EAP pattern. The results confirm that changes in the intensity and location of anomalous diabatic heating can both alter the EAP pattern and ultimately influence the NSWSP-EAP linkage. In particular, weakening of the heating anomaly over regions from the Indochina Peninsula to the Philippines can diminish the EAP signal across East Asia by reducing the intensity of the anomalous anticyclone over regions from the North Indian Peninsula to the Subtropical Western Pacific and of the anomalous cyclone covering regions from North China to southern Japan (Figs. 7a, b and e). The westward shift of the heating anomaly relative to the Philippines can also weaken the EAP signal across East Asia by shifting the anomalous anticyclone at lower latitudes eastward and reducing the intensity of the anomalous cyclone at middle latitudes (Figs. 7c, d and f). These results indicate that changes in the intensity and position of diabatic heating anomalies across regions from the Indochina Peninsula eastward to the Central Pacific affect the EAP pattern through different mechanisms. Nonetheless, both anomaly types weaken the EAP signal across East Asia, ultimately disconnecting the NSWSP and EAP patterns.

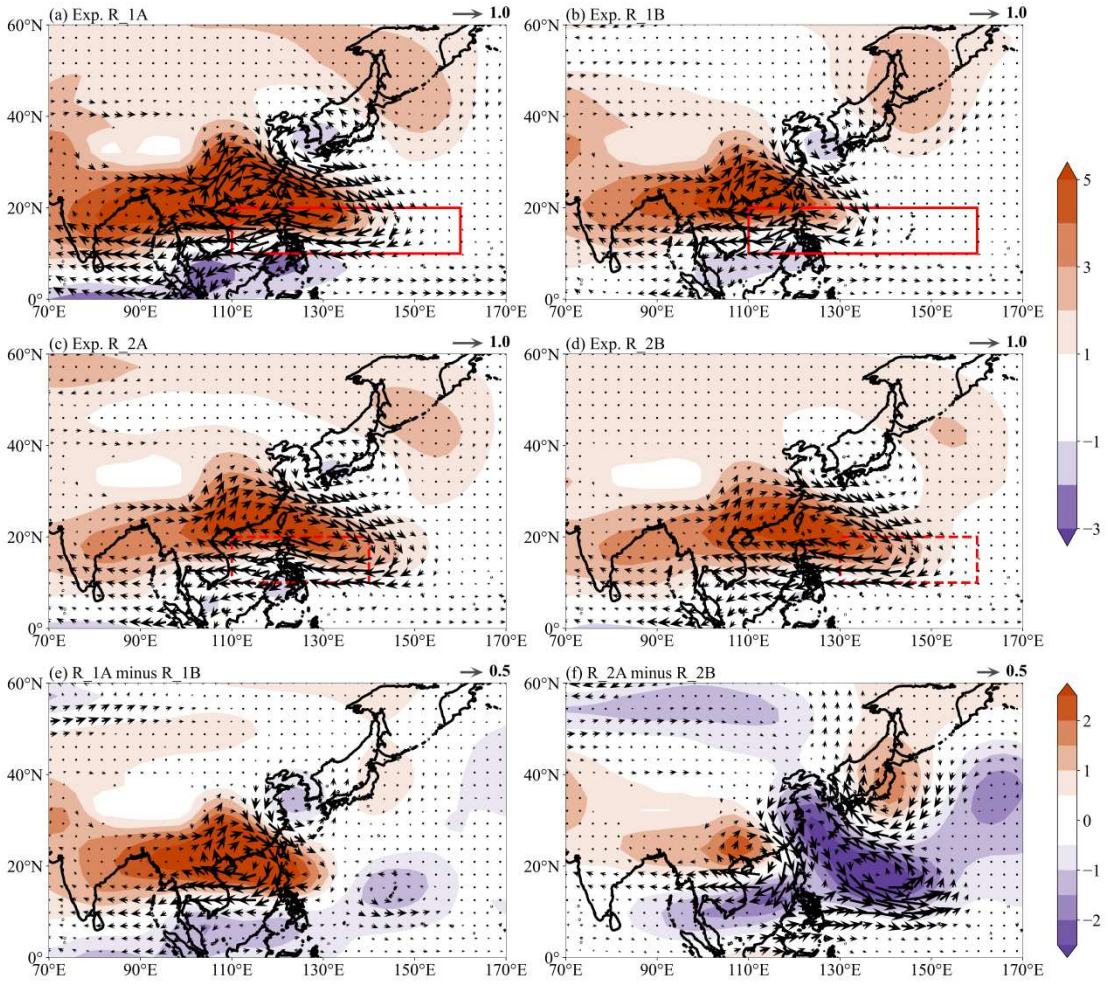


Fig. 7 Response of the 700 hPa horizontal winds (vectors; m s^{-1}) and the 500 hPa stream function (shading; 10^5 m^2 s^{-1}) to anomalous diabatic heating in the region 10°N–20°N, 110°E–160°E associated with the EAP pattern during (a) epoch 1 and (b) epoch 2. (c) and (d) are as in (a) and (b), respectively, but for anomalous diabatic heating in 10°N–20°N, 110°E–140°E during epoch 1 and in 10°N–20°N, 130°E–160°E during epoch 2. (e) and (f) show the differences between the results in (a) and (b), and in (c) and (d), respectively.

4. Discussion

To confirm that the interdecadal change in the NSWSP-EAP relationship is not sensitive to the choice of EAP index, we also calculated EAP indices using the methods of Huang (2004), Kosaka and Nakamura (2010), and Wu et al. (2013). As with the index of Xie et al. (2016), the other EAP indices also show a notable interdecadal change around the early 2000s. In particular, the indices of Kosaka and Nakamura (2010) and Wu et al. (2013) show the same change point as that of Xie et al. (2016), whereas the index of Huang (2004) shows a change two years earlier. Overall, all four indices show an interdecadal shift from significant to insignificant correlations with NSWSP.

By comparing variations in atmospheric circulation and heating fields associated with the NSWSP and EAP across the two periods, we identified that the eastward shift of EAP-related anomalous circulation, driven by changes in diabatic heating anomalies from the Indochina Peninsula to the Central Pacific, is the key factor underlying interdecadal changes in the NSWSP-EAP relationship. These conclusions are consistent with Xu et al. (2019), who also noted an eastward shift of the EAP pattern in the late 1990s and attributed it primarily to a shift in the EAP excitation location. We further investigated how changes in the intensity and location of tropical diabatic heating anomalies influence the EAP pattern. Our results show a similarly diminished EAP signal over East Asia, but via a different process. This implies that an eastward shift in the excitation location may not be the only way to diminish the EAP signal over East Asia. Our analysis also reveals that anomalous circulation around the South China Sea serves as a key link between the NSWSP and the EAP pattern, a finding that can be inferred from and corroborated by previous research. For instance, He and Wu (2018) found that the correlation of summer precipitation between the western North Pacific and the South China Sea has weakened since the early 2000s. Similarly, Lu et al. (2022) observed a diminished influence of the EAP pattern on interannual variability in summer rainfall over South China since the mid-2000s. Both studies noted a weakening and eastward shift of the low-level anomalous circulation system at lower latitudes during periods of weak connection. In other words, during strong connections, the anomalous circulation system at lower latitudes tends to be positioned further westward, covering the South China Sea, but it shifts eastward as the connection weakens.

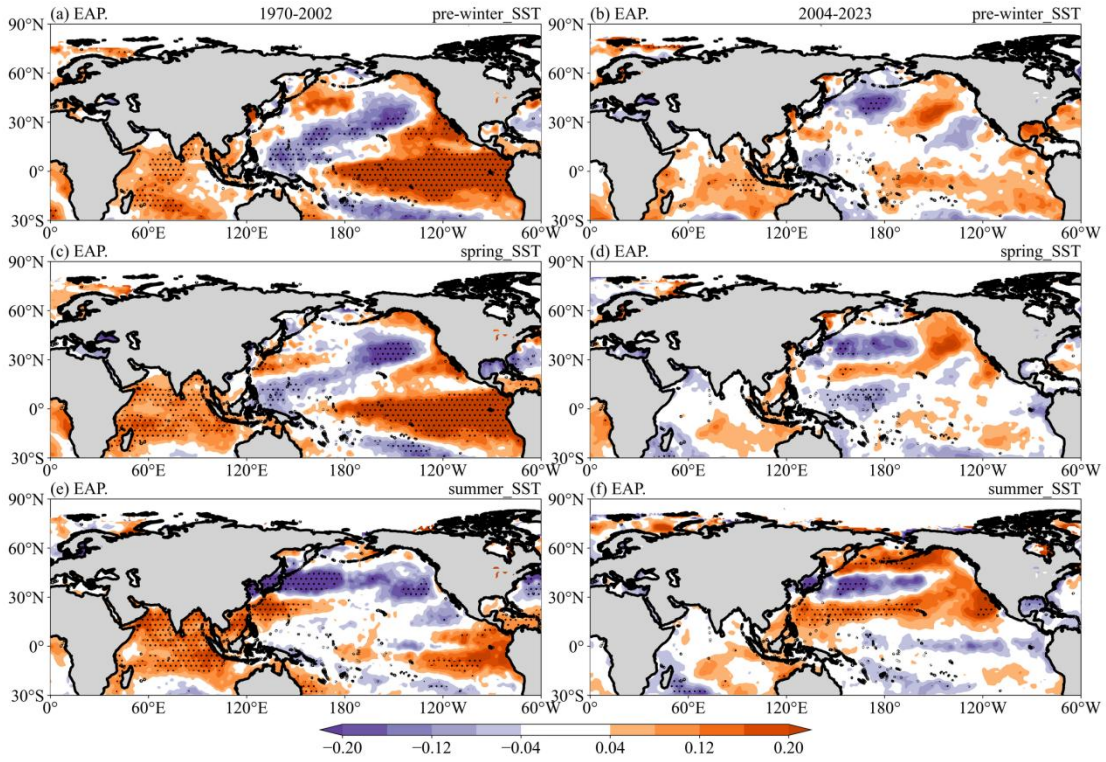


Fig. 8 Regression of sea surface temperature anomalies (°C) in (a) the previous winter, (c) the previous spring, and (e) the simultaneous summer onto the standardized EAP index during epoch 1. (b), (d), and (f) are as (a), (c), and (e), respectively, but for epoch 2. Shaded areas with dots denote statistical significance at the 90% confidence level for the t-test.

Regarding the interdecadal change in the EAP pattern around the 2000s, there remains no consensus on either the change in the pattern itself or its external forcing. In addition to the eastward shift around the early 2000s, some studies also noted an interdecadal weakening of the tropical-subtropical linkage within the EAP structure (e.g., Li and Lu 2020; Sun et al. 2024). Current research on this interdecadal change generally agrees that the influence of the IOBM has weakened. However, some studies attribute this shift to changes in El Niño type (Xu et al. 2019; Li and Lu 2020; Lu et al. 2022), while others attribute it to accelerated ENSO evolution (Sun et al. 2024; Yu et al. 2025). Our results indicate a decreased influence of EP El Niño on the EAP pattern since the early 2000s, but no increase in the impact of CP El Niño (Fig. 8; Table 1). Regressing SSTAs on the standardized EAP indices from epoch 1 (Figs. 8a, c and e) to epoch 2 (Figs. 8b, d and f) shows that the strong influence of the EP El Niño-IOBM chain, illustrated by the capacitor effect, has disappeared. Simultaneously, the notable positive SSTAs in the western Pacific during summer shifted eastward and extended further. Changes in EAP-related anomalous circulation and Indo-Pacific

SSTAs, together with changes in their correlations with the WPSH indices (Table 1), indicate that the EAP pattern has become isolated from the ENSO-East Asian summer monsoon system since the early 2000s. These results raise another question about the summertime air-sea interaction driving the EAP wave train: did the dominant role shift from ocean processes in the first period to atmospheric processes in the second? In addition, beyond changes in ENSO type and evolution and the diminished Indian Ocean capacitor effect, further work should assess whether other factors also contributed to interdecadal variations in the EAP pattern. These include the interdecadal change or linear trend in the Indo-Pacific (Zhao et al. 2021; Han and Wu 2026), changes in the Maritime Continent's response to diabatic heating anomalies (Xu and Guan 2019), and signals from the middle and high latitudes, such as Rossby wave activity in the westerlies (Xie et al. 2022; Huang et al. 2025) or Arctic sea ice forcing (Zhang et al. 2024).

Table 1 Correlation coefficients among summer precipitation in northern Southwest China, the EAP index, and various climate indices across the two epochs

Indices	**NSWSP**		**EAP**	
	epoch 1	epoch 2	epoch 1	epoch 2
IOBM	0.24	0.49*	0.53*	0.14
NINO3	0.33	0.32	0.43*	0.03
NINO4	0.11	0.37	0.33	0.07
AREA	0.55*	0.36	0.56*	0.10
INT	0.59*	0.35	0.56*	0.05
WRP	-0.34	-0.13	-0.37*	-0.23

* Indicates statistical significance at the 95% confidence level. The NINO indices are from the previous winter, while the others are simultaneous. AREA, INT, and WRP represent the area, intensity, and the western ridge point of the Western Pacific Subtropical High, respectively.

When EAP impacts were weaker, interannual variation in summer rainfall decreased across eastern China, including the Yangtze-Huai River valley and South China. Conversely, it became more pronounced in northern Southwest China. Unlike the EAP pattern, which detached from both types of El Niño and IOBM, the notable relationship between NSWSP and tropical Pacific SSTAs shifted from the eastern regions (Figs. 9a, c, and e) to the central areas (Figs. 9b, d, and f) during the previous winter and spring. Additionally, its connection with northern Indian Ocean SSTAs

diminished on the eastern side but increased on the western side during summer. Apparently, the East Asian summer monsoon, which plays a dominant role in modulating summer precipitation in eastern China, has exhibited a diminished response to the strongest external interannual signal (ENSO) since the early 2000s. As a result, interannual variation in summer precipitation over eastern China has decreased. By contrast, a significant change in the related Indo-Pacific SSTA forcing could alter the fundamental framework by which three monsoon systems jointly influence summer precipitation in Southwest China, thereby increasing precipitation variability in Southwest China.

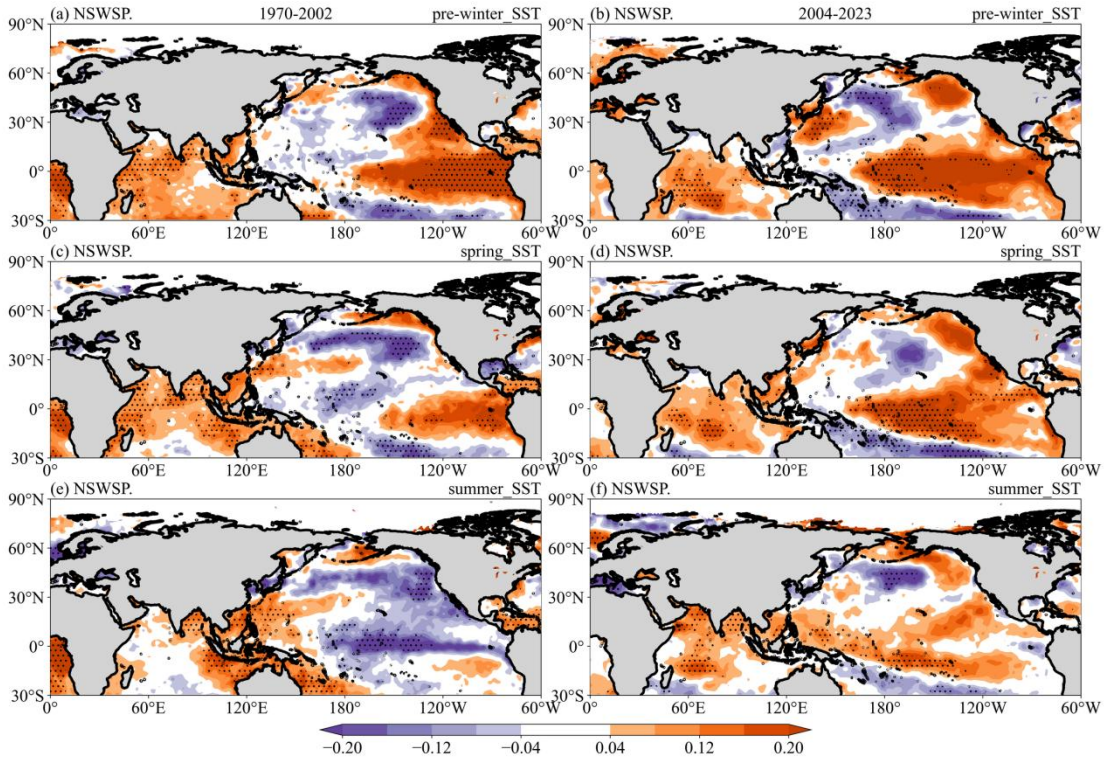


Fig. 9 Same as Fig. 8, but for the regression onto standardized summer precipitation in northern Southwest China.

5. Conclusions

This study examined the interdecadal shift in the NSWSP-EAP relationship around the early 2000s. Before 2003, we observed significant correlations between summer rainfall in northern Southwest China and the EAP pattern. From 2004 onward, this correlation disappeared, coinciding with increased interannual variability of the NSWSP and decreased variability of the EAP pattern. To address this, we conducted dynamical diagnostics and numerical experiments. Our main findings are summarized below:

1) The interdecadal change in the NSWSP-EAP link mainly resulted from the eastward shift of the anomalous circulation induced by the EAP pattern around the early 2000s. In epoch 1 (1970–2002), northern Southwest China was jointly affected by EAP-driven anomalous anticyclonic circulation from the Indochina Peninsula to the subtropical western Pacific and anomalous cyclonic circulation from North China to Japan. These two systems facilitated the transport of anomalous moisture from the South China Sea and the western Pacific to northern Southwest China, producing anomalous low-level convergence there. In epoch 2 (2004–2023), however, these two circulation systems weakened and shifted further east, thereby losing their direct influence on northern Southwest China.

2) Variations in anomalous diabatic heating across regions from the Indochina Peninsula eastward to the Central Pacific can explain the interdecadal change in the EAP pattern. From epoch 1 to epoch 2, diabatic heating anomalies west of the Philippines decreased markedly, while those east of the Philippines increased slightly, preventing westward extension of EAP-related anomalous circulation and resulting in a weakened, eastward-shifted EAP wave train. Numerical experiments further confirm that decreasing diabatic heating anomalies from the Indochina Peninsula to the Philippines reduces the intensity of the anomalous anticyclone over the North Indian Peninsula to the Subtropical western Pacific and the anomalous cyclone over North China to southern Japan. Shifting the heating anomaly from west of the Philippines to the east shifts the anomalous anticyclone at lower latitudes eastward and weakens the anomalous cyclone at middle latitudes. Together, these changes weaken the EAP signal across East Asia, ultimately disconnecting the NSWSP from the EAP pattern.

3) Anomalous circulations around the South China Sea bridge the NSWSP-EAP linkage. During the period of strong NSWSP-EAP connection, the tropical diabatic heating anomaly that excites the EAP pattern is stronger and located farther west. Consequently, EAP-related anomalous circulations are more intense and extend farther west, favoring WPSH intensification and westward extension. As a result, anomalous anticyclonic circulation around the South China Sea in the middle and lower troposphere can be observed, facilitating summer precipitation over northern Southwest China. Conversely, during the period of weak NSWSP-EAP connection, the anomalous diabatic heating center that excites the EAP pattern shifts farther east. This leads to a weaker, more eastward-located EAP pattern that exerts less influence

on the WPSH and the anomalous circulation over the South China Sea, resulting in a poor connection between the EAP pattern and both the NSWSP and the WPSH.

References

Bi W, Li M, Weng B, et al. (2023) Drought-flood abrupt alteration events over China. Sci Total Environ 875:162529. https://doi.org/10.1016/j.scitotenv.2023.162529

Ding Y, Chan J C L (2005) The East Asian summer monsoon: an overview. Meteorol Atmos Phys 89(1):117–142. https://doi.org/10.1007/s00703-005-0125-z

Dong Z, Yang R, Zheng C, et al. (2025) A warming-drying climate hits Yunnan, Southwest China, during the past half century. Clim Dyn 63(8):335. https://doi.org/10.1007/s00382-025-07806-5

Fujinami H, Yasunari T (2009) The effects of midlatitude waves over and around the Tibetan Plateau on submonthly variability of the East Asian summer monsoon. Mon Weather Rev 137(7):2286–2304. https://doi.org/10.1175/2009mwr2826.1

Han S, Wu Z (2026) Ocean memory loss in the maritime continent: a dual influence of natural decadal oscillations and human-induced warming. Clim Dyn 64(2):52. https://doi.org/10.1007/s00382-025-08037-4

He Z, Wu R (2018) Change in coherence of interannual variability of summer rainfall over the western Pacific around the early 2000s: Role of Indo-Pacific ocean forcing. J Clim 31(9):3525–3538. https://doi.org/10.1175/jcli-d-17-0687.1

Hersbach H, Bell B, Berrisford P, et al. (2020) The ERA5 global reanalysis. Q J R Meteorol Soc 146(730):1999–2049. https://doi.org/10.1002/qj.3803

Hu J, Miao C, Su J, et al. (2025) An upgraded high-precision gridded precipitation dataset for the Chinese mainland considering spatial autocorrelation and covariates. Earth Syst Sci Data 17(8):3987–4004. https://doi.org/10.5194/essd-17-3987-2025

Hu P, Chen W, Chen S, et al. (2024) Revisiting the linkage between the Pacific-Japan pattern and Indian summer monsoon rainfall: The crucial role of the Maritime Continent. Geophys Res Lett 51(3):e2023GL106982. https://doi.org/10.1029/2023gl106982

Huang G (2004) An index measuring the interannual variation of the East Asian summer monsoon—The EAP index. Adv Atmos Sci 21(1):41–52. https://doi.org/10.1007/bf02915679

Huang K, Zeng G, Datti A D, et al. (2025) Influence of the East Asia-Pacific and Eurasian teleconnection on the summer marine heatwaves in the Japan/East Sea. Weather Clim Extrem 49:100783. https://doi.org/10.1016/j.wace.2025.100783

Huang R, Li W (1987) Influence of the heat source anomaly over the tropical western

Pacific on the subtropical high over East Asia. In: Proceedings of the International Conference on the General Circulation of East Asia, Chengdu, China, pp 40–45

Huang R, Li W (1988) Influence of the heat source anomaly over the tropical western Pacific on the subtropical high over East Asia and its physical mechanism. Chin J Atmos Sci 14:95–107 (in Chinese)

Huang R, Sun F (1992) Impacts of the tropical western Pacific on the East Asian summer monsoon. J Meteorol Soc Jpn 70(1B):243–256. https://doi.org/10.2151/jmsj1965.70.1B_243

Huangfu J, Chen W, Ma T, et al. (2018) Influences of sea surface temperature in the tropical Pacific and Indian Oceans on tropical cyclone genesis over the western North Pacific in May. Clim Dyn 51(5):1915–1926. https://doi.org/10.1007/s00382-017-3989-y

Kosaka Y, Nakamura H (2006) Structure and dynamics of the summertime Pacific-Japan teleconnection pattern. Q J R Meteorol Soc 132(619):2009–2030. https://doi.org/10.1256/qj.05.204

Kosaka Y, Nakamura H (2010) Mechanisms of meridional teleconnection observed between a summer monsoon system and a subtropical anticyclone. Part I: The Pacific-Japan pattern. J Clim 23(19):5085–5108. https://doi.org/10.1175/2010jcli3413.1

Kosaka Y, Takaya Y, Kamae Y (2021) The Indo-western Pacific Ocean capacitor effect. In: Tropical and extratropical air-sea interactions. Elsevier, pp 141–169. https://doi.org/10.1016/B978-0-12-818156-0.00012-5

Kubota H, Kosaka Y, Xie S P (2016) A 117-year long index of the Pacific-Japan pattern with application to interdecadal variability. Int J Climatol 36(4):1575–1589. https://doi.org/10.1002/joc.4441

Li L, Zhai P, Chen Y, et al. (2016) Low-frequency oscillations of the East Asia-Pacific teleconnection pattern and their impacts on persistent heavy precipitation in the Yangtze-Huai River valley. J Meteorol Res 30(4):459–471. https://doi.org/10.1007/s13351-016-6024-z

Li M, Zhao Y, Long Y, et al. (2025) Interannual variations in extreme wet spells and their potential causes in Southwest China. Atmos Res 323:108194. https://doi.org/10.1016/j.atmosres.2025.108194

Li X, Li S, Wang L, et al. (2026) Spatiotemporal variability of drought-flood abrupt alternation events in Southwest China during 1961 to 2024. Theor Appl Climatol 157(2):96. https://doi.org/10.1007/s00704-026-06024-1

Li X, Lu R (2020) Breakdown of the summertime meridional teleconnection pattern over the western North Pacific and East Asia since the early 2000s. J Clim 33(19):8487–8505. https://doi.org/10.1175/jcli-d-19-0746.1

Li Z, Ren H L, Lu M, et al. (2024) Interannual variations of westward extension area of western Pacific subtropical high and its relationship with precipitation in

643 East Asia. Atmos Res 298:107148.
644 https://doi.org/10.1016/j.atmosres.2023.107148
645 Liebmann B, Smith C A (1996) Description of a complete (interpolated) outgoing
646 longwave radiation dataset. Bull Am Meteorol Soc 77(6):1275–1277.
647 https://doi.org/10.1175/1520-0477(1996)077<1275:DOACIO>2.0.CO;2
648 Lin X, Wang L, Gao J, et al. (2021) Intraseasonal variability of the east Asia-Pacific
649 teleconnection and its impacts on multiple tropical cyclone genesis over the
650 Western North Pacific. Front Earth Sci 8:598043.
651 https://doi.org/10.3389/feart.2020.598043
652 Lin Z, Bueh C (2021) Formation of the northern East Asian low: role of diabatic
653 heating. Clim Dyn 56(9–10):2839–2854.
654 https://doi.org/10.1007/s00382-020-05615-6
655 Liu B, Wu G, Mao J, et al. (2013) Genesis of the South Asian high and its impact on
656 the Asian summer monsoon onset. J Clim 26(9):2976–2991.
657 https://doi.org/10.1175/jcli-d-12-00286.1
658 Liu D, Wang L, Guan Z, et al. (2024) Maintenance mechanism for the summertime+
659 EAP/-SR combination pattern. Clim Dyn 62(7):6555–6578.
660 https://doi.org/10.1007/s00382-024-07224-z
661 Liu K, Chen J, Zhou L T, et al. (2022) Interdecadal change in autumn rainfall over
662 Southeast China and its association with tropical Pacific SST. Theor Appl
663 Climatol 150(3):1545–1557. https://doi.org/10.1007/s00704-022-04249-4
664 Lu W, Zhu Y, Zhong Z, et al. (2022) Weakened impacts of the East Asia-Pacific
665 teleconnection on the interannual variability of summertime precipitation over
666 South China since the mid-2000s. Remote Sens 14(20):5098.
667 https://doi.org/10.3390/rs14205098
668 Luo J, Yang A (2024) Analysis of change in summer extreme precipitation in
669 Southwest China and human adaptation. Sustainability 16(17):7329.
670 https://doi.org/10.3390/su16177329
671 Ma Z F, Liu J, Zhang S Q, et al. (2013) Observed climate changes in southwest China
672 during 1961–2010. Adv Clim Chang Res 4(1):30–40.
673 https://doi.org/10.3724/sp.j.1248.2013.030
674 Nitta T (1987) Convective activities in the tropical western Pacific and their impact
675 on the Northern Hemisphere summer circulation. J Meteorol Soc Jpn
676 65(3):373–390. https://doi.org/10.2151/jmsj1965.65.3_373
677 Noh E, Kim J, Jun S Y, et al. (2023) Atmospheric pathway of marine heatwaves over
678 the Northwestern Pacific. Sci Rep 13(1):22821.
679 https://doi.org/10.1038/s41598-023-49833-4
680 Qiu J, He C, Liu X, et al. (2024) Projecting dry-wet abrupt alternation across China
681 from the perspective of soil moisture. npj Clim Atmos Sci 7(1):269.
682 https://doi.org/10.1038/s41612-024-00808-w
683 Qu X, Huang G (2012) Impacts of tropical Indian Ocean SST on the meridional

displacement of East Asian jet in boreal summer. Int J Climatol 32(13):2073–2080. https://doi.org/10.1002/joc.2378

Rayner N A, Parker D E, Horton E B, et al. (2003) Global analyses of sea surface temperature, sea ice, and night marine air temperature since the late nineteenth century. J Geophys Res Atmos 108(D14):4407. https://doi.org/10.1029/2002jd002670

Shang W, Li S, Ren X, et al. (2020) Event-based extreme precipitation in central-eastern China: Large-scale anomalies and teleconnections. Clim Dyn 54(3):2347–2360. https://doi.org/10.1007/s00382-019-05116-1

Song J, Klotzbach P J, Wang Y F, et al. (2025) Seasonality in the ENSO-independent influence of tropical Indian Ocean sea surface temperature anomalies on western North Pacific tropical cyclone genesis. J Meteorol Soc Jpn 103(2):257–278. https://doi.org/10.2151/jmsj.2025-013

Su J, Ding Y, Liu Y, et al. (2024) China is suffering from fewer but more severe drought to flood abrupt alternation events. Weather Clim Extrem 46:100737. https://doi.org/10.1016/j.wace.2024.100737

Sun B, Li H, Wang H, et al. (2026) Impact of ENSO on Meiyu-Baiu-Changma rains: Processes, mechanisms, modeling, and future challenges. Rev Geophys 64(1):e2025RG000890. https://doi.org/10.1029/2025rg000890

Sun X, Li Q, Wu Q (2024) Mechanisms of early and late summer precipitation in Southwest China: dynamic and thermodynamic processes. Clim Dyn 62(8):7907–7925. https://doi.org/10.1007/s00382-024-07314-y

Sun Y, Xu H M, Deng J C (2014) Interdecadal variation in Pacific-Japan teleconnection patterns and possible causes. Chin J Atmos Sci 38(6):1055–1065 (in Chinese)

Sun Y, Zhu Z, Yang Y, et al. (2024) Decadal change in the connection between the Pacific-Japan pattern and the Indian Ocean SST basin mode. Clim Dyn 62(5):4281–4296. https://doi.org/10.1007/s00382-024-07132-2

Tao L, Li T, Ke Y H, et al. (2017) Causes of interannual and interdecadal variations of the summertime Pacific-Japan-like pattern over East Asia. J Clim 30(22):8845–8864. https://doi.org/10.1175/jcli-d-15-0817.1

Tao Y, Cao J, Lan G, et al. (2016) The zonal movement of the Indian-East Asian summer monsoon interface in relation to the land-sea thermal contrast anomaly over East Asia. Clim Dyn 46(9–10):2759–2771. https://doi.org/10.1007/s00382-015-2729-4

Wang B, Wu R, Fu X (2000) Pacific-East Asian teleconnection: how does ENSO affect East Asian climate? J Clim 13(9):1517–1536. https://doi.org/10.1175/1520-0442(2000)013<1517:peathd>2.0.co;2

Wang C, Chen C, Zhang S, et al. (2023) Variation characteristics of extreme climate events in Southwest China from 1961 to 2017. Heliyon 9(9):e19648. https://doi.org/10.1016/j.heliyon.2023.e19648

Wang H, Li Z, Li J, et al. (2023) Interannual variation in the East Asian summer monsoon-tropical Atlantic SST relationship modulated by the Interdecadal Pacific Oscillation. npj Clim Atmos Sci 6(1):169. https://doi.org/10.1038/s41612-023-00497-x

Wang L, Gui S, Cao J, et al. (2018) Summer precipitation anomalies in the low-latitude highlands of China coupled with the subtropical Indian Ocean dipole-like sea surface temperature. Clim Dyn 51(7):2773–2791. https://doi.org/10.1007/s00382-017-4044-8

Wang L, Xu P (2024) Waveguide teleconnections in the boreal summer: Progress and perspectives. Chin J Atmos Sci 48(1):287–304 (in Chinese)

Wang Q, Zhai P, Zhang Q (2025) Regional patterns of climate change and extreme events in China since 1961. J Meteorol Res 39(3):688–697. https://doi.org/10.1007/s13351-025-4901-z

Wang S, Zuo H (2016) Effect of the East Asian westerly jet's intensity on summer rainfall in the Yangtze River valley and its mechanism. J Clim 29(7):2395–2406. https://doi.org/10.1175/jcli-d-15-0259.1

Watanabe M, Kimoto M (2000) Atmosphere-ocean thermal coupling in the North Atlantic: A positive feedback. Q J R Meteorol Soc 126(570):3343–3369. https://doi.org/10.1002/qj.49712657017

Wu B, Li T, Zhou T (2010) Relative contributions of the Indian Ocean and local SST anomalies to the maintenance of the western North Pacific anomalous anticyclone during the El Niño decaying summer. J Clim 23(11):2974–2986. https://doi.org/10.1175/2010jcli3300.1

Wu H, An X, Sun Y, et al. (2026) Dry and wet alternation events in China during 1961–2020. J Meteorol Res 40(2):361–375. https://doi.org/10.1007/s13351-026-5183-9

Wu J, Gao X J (2013) A gridded daily observation dataset over China region and comparison with the other datasets. Chin J Geophys 56(4):1102–1111 (in Chinese)

Wu J, Xu X F, Jin F F, Guo P W (2013) Research of the intraseasonal evolution of the East Asia Pacific pattern and the maintenance mechanism. Acta Meteorol Sin 71:476–491 (in Chinese)

Xiao C, Wu P, Zhang L, et al. (2018) Increasing flash floods in a drying climate over Southwest China. Adv Atmos Sci 35(8):1094–1099. https://doi.org/10.1007/s00376-018-7275-7

Xie M, Wang C, Chen S (2022) The role of the Maritime Continent SST anomalies in maintaining the Pacific-Japan pattern on decadal time scales. J Clim 35(3):1079–1095. https://doi.org/10.1175/jcli-d-21-0555.1

Xie Q, Gu X, Li G, et al. (2022) Variation characteristics of rainstorms and floods in southwest China and their relationships with atmospheric circulation in the summer half-year. Atmosphere 13(12):2103.

https://doi.org/10.3390/atmos13122103

Xie S P, Hu K, Hafner J, et al. (2009) Indian Ocean capacitor effect on Indo-western Pacific climate during the summer following El Niño. J Clim 22(3):730–747. https://doi.org/10.1175/2008jcli2544.1

Xie S P, Kosaka Y, Du Y, et al. (2016) Indo-western Pacific Ocean capacitor and coherent climate anomalies in post-ENSO summer: A review. Adv Atmos Sci 33(4):411–432. https://doi.org/10.1007/s00376-015-5192-6

Xu H, Chen H, Wang H (2021) Interannual variation in summer extreme precipitation over Southwestern China and the possible associated mechanisms. Int J Climatol 41(6):3425–3438. https://doi.org/10.1002/joc.7027

Xu P, Wang L, Chen W, et al. (2019) Structural changes in the Pacific-Japan pattern in the late 1990s. J Clim 32(2):607–621. https://doi.org/10.1175/jcli-d-18-0123.1

Xu Q, Guan Z (2019) Interdecadal change of diabatic forcing over key region of the Maritime Continent and its possible relations with the East Asian summer monsoon anomalies. J Trop Meteorol 25(1):54–62.

Yan H M, Wang L (2019) The relationship between east-west movement of subtropical high over Northwestern Pacific and precipitation in Southwestern China. J Appl Meteorol Sci 30(3):360–375 (in Chinese)

Yanai M, Esbensen S, Chu J H (1973) Determination of bulk properties of tropical cloud clusters from large-scale heat and moisture budgets. J Atmos Sci 30(4):611–627. https://doi.org/10.1175/1520-0469(1973)030<0611:dobpot>2.0.co;2

Yang J, Liu Q, Xie S P, et al. (2007) Impact of the Indian Ocean SST basin mode on the Asian summer monsoon. Geophys Res Lett 34(2):L02708. https://doi.org/10.1029/2006gl028571

Yang M X, Xiao T G, Zhao P, et al. (2022) Joint effect of East Asia-Pacific and Scandinavian teleconnections on summer precipitation in Southwest China. Theor Appl Climatol 150(3):1477–1493. https://doi.org/10.1007/s00704-022-04227-w

Yang W, Li X, Wang L, et al. (2025) Remote effect of tropical South Atlantic variability on the Pacific-Japan pattern. Clim Dyn 63(6):255. https://doi.org/10.1007/s00382-025-07718-4

Yu J, Li Q, Ding Y, et al. (2026) Predominant circulation patterns affecting regional persistent extreme heavy rainfall over the Huaihe River Basin of China in July and their formation mechanisms. J Clim 39(4):1155–1182. https://doi.org/10.1175/jcli-d-24-0525.1

Yu T, Chen W, Huang P, et al. (2025) Weakened influence of ENSO on the East Asian summer monsoon since the early 2000s. npj Clim Atmos Sci 8(1):114. https://doi.org/10.1038/s41612-025-00983-4

Yu Y, You Q, Zuo Z, et al. (2023) Compound climate extremes in China: Trends,

causes, and projections. Atmos Res 286:106675. https://doi.org/10.1016/j.atmosres.2023.106675

Yuan J, Zhao D, Yang R, et al. (2018) Predecessor rain events over China's low-latitude highlands associated with Bay of Bengal tropical cyclones. Clim Dyn 50(3):825–843. https://doi.org/10.1007/s00382-017-3643-8

Zhang C (2020) Moisture sources for precipitation in Southwest China in summer and the changes during the extreme droughts of 2006 and 2011. J Hydrol 591:125333. https://doi.org/10.1016/j.jhydrol.2020.125333

Zhang C, Tang Q, Chen D, et al. (2017) Tracing changes in atmospheric moisture supply to the drying Southwest China. Atmos Chem Phys 17(17):10383–10393. https://doi.org/10.5194/acp-17-10383-2017

Zhang M, Li J, Li N, et al. (2025) Spatiotemporal characteristics and associated circulation patterns of warm-season precipitation in a complex terrain region of Southwest China. Clim Dyn 63(2):103. https://doi.org/10.1007/s00382-024-07581-9

Zhang X, He B, Bao Q, et al. (2024) The role of Arctic sea ice loss in the interdecadal trends of the East Asian summer monsoon in a warming climate. npj Clim Atmos Sci 7(1):174. https://doi.org/10.1038/s41612-024-00717-y

Zhao X, Dong B, Lu R (2021) Interdecadal weakening of the cross-equatorial flows over the Maritime Continent during the boreal summer in the mid-1990s: drivers and physical processes. Clim Dyn 57(1):55–72. https://doi.org/10.1007/s00382-021-05692-1

Zheng G, Li Y, Chen Q, et al. (2022) The increasing predominance of extreme precipitation in Southwest China since the late 1970s. Atmos Ocean Sci Lett 15(5):100227. https://doi.org/10.1016/j.aosl.2022.100227

Zhi R, Feng T, Dong W, et al. (2025) Interdecadal variation in the relationship between ENSO and summer precipitation in the middle and lower reaches of the Yangtze River. Clim Dyn 63(4):177. https://doi.org/10.1007/s00382-025-07606-x

Statements and Declarations

Funding

This work was jointly supported by the Natural Science Foundation of Yunnan Province (Grant No. 202302AN360006) and the National Natural Science Foundation of China (Grant No. 42175042).

Competing interests

The authors declare that they have no known competing financial interests or

personal relationships that could have appeared to influence the work reported in this paper.

Ethics approval

This study does not involve human participants or animals.

Consent to participate and for publication

Not applicable.

Authorship contribution statement

All authors contributed to the study. Jieliang Wei: investigation, visualization, and writing – original draft. Minggang Li: conceptualization, methodology, and writing – original draft. Haolin Luo: conceptualization and numerical experiments. Yong Zhao: conceptualization and methodology. Pengguo Zhao and Yang Li reviewed and further optimized the study.

Data availability statement

The CHM_PRE V2 precipitation dataset is publicly available from the Zenodo repository at https://doi.org/10.5281/zenodo.14632157 (Hu et al. 2025). The ERA5 monthly mean reanalysis dataset is from the European Center for Medium-Range Weather Forecasts (https://cds.climate.copernicus.eu/). The WPSH indices are provided by the National Climate Centre of the China Meteorological Administration (http://cmdp.ncc-cma.net/Monitoring/cn_index_130.php). The OLR data are provided by the NOAA/OAR/ESRL Physical Sciences Laboratory (https://psl.noaa.gov/data/gridded/). The HadISST dataset is provided by the UK Met Office Hadley Centre (https://www.metoffice.gov.uk/hadobs/hadisst/).